

Oxygen Chain Disorder as the Weak Scattering Source in $\text{YBa}_2\text{Cu}_3\text{O}_{6.50}$

J. S. Bobowski,¹ P. J. Turner,^{1,2} R. Harris,^{1,3} Ruixing Liang,¹ D. A. Bonn,¹ and W. N. Hardy¹

¹*Department of Physics and Astronomy, University of British Columbia, 6224 Agricultural Road, Vancouver, British Columbia, Canada V6T 1Z1*

²*Department of Physics, Simon Fraser University,*

8888 University Drive, Burnaby, British Columbia, Canada, V5A 1S6

³*D-Wave Systems Inc., 4401 Still Creek Drive, Burnaby, British Columbia, Canada, V5C 6G9*

(Dated: October 30, 2018)

The microwave conductivity of an ultra-pure single crystal of $\text{YBa}_2\text{Cu}_3\text{O}_{6.50}$ has been measured deep in the superconducting state as a continuous function of frequency from 0.5 \rightarrow 20 GHz. Conductivity spectra were first measured at four temperatures below 10 K after having prepared the crystal in the so called ortho-II phase in which the CuO chain oxygen are ordered into alternating full and empty chains. These spectra exhibit features expected for quasiparticle scattering from dilute weak impurities (small scattering phaseshift) in an otherwise clean d -wave superconductor. The measurements were repeated on the same crystal after heating and then rapidly quenching the sample to reduce the degree of oxygen order in the CuO chains. With the increased disorder, the conductivity spectra retain the distinctive weak-limit scattering features, but have increased widths reflecting an increase in quasiparticle scattering. These measurements unambiguously establish that CuO chain oxygen disorder is the dominant source of in-plane quasiparticle scattering in high purity YBCO.

Disorder and inhomogeneity play crucial roles in determining the behaviour of many measurable properties of the cuprates. Early on, cation substitution in the CuO_2 planes was found to have striking effects on low temperature properties such as the magnetic penetration depth^{1,2}, and scanning tunneling spectroscopy (STS) has provided detailed tests of the influence of point-like defects on d -wave superconductors³. More recently, attention has been focused upon the puzzling effects of off-plane disorder. Fujita *et al.* have shown that off-plane cation disorder has a substantial impact on the critical temperature T_c ⁴. STS measurements by McElroy *et al.* on $\text{Bi}_2\text{Sr}_2\text{CaCu}_2\text{O}_{8+\delta}$ (BSCCO) have provided evidence that interstitial dopant oxygen atoms are correlated with mesoscale variation in the electronic spectrum⁵. In this context $\text{YBa}_2\text{Cu}_3\text{O}_{6+y}$ (YBCO) offers a unique opportunity to study the influence of defects, since high purity crystals of YBCO can be grown with negligible cation disorder both on- and off-plane⁶. Like BSCCO, YBCO's doping can be controlled via off-plane oxygen atoms, but in YBCO these dopants are organized into CuO_y chains whose filling and degree of disorder can be systematically manipulated⁷. For instance, $\text{YBa}_2\text{Cu}_3\text{O}_7$ has filled CuO chains that provide a slightly overdoped 85 K superconductor with very low disorder. At $y = 0.5$ one can prepare a stable phase with alternating filled and empty CuO chains (ortho-II superstructure) that also can have very little disorder⁸. Above 100°C, the ortho-II phase gives way to the ortho-I phase in which all CuO chains are equally occupied. Because oxygenation of YBCO is negligibly slow below 300°C, a low-temperature anneal at 200°C followed by a rapid quench can change the level of disorder in the CuO chains without changing the total oxygen content⁷. In this article, we demonstrate that oxygen disorder in the CuO chains is the dominant source of quasiparticle scattering at low temperature in

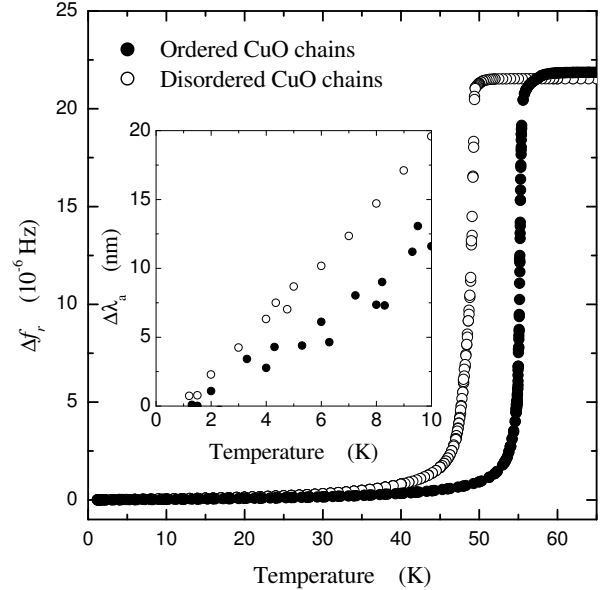


FIG. 1: Measured change in the resonant frequency of the 900 MHz cavity when loaded with $\text{YBa}_2\text{Cu}_3\text{O}_{6.50}$ with ordered (solid points) and disordered (hollow points) CuO chains. The sample is oriented such that currents propagate in the \hat{a} -axis direction. Inset: The low-temperature $\Delta\lambda_a(T)$ after removing the \hat{c} -axis contribution.

$\text{YBa}_2\text{Cu}_3\text{O}_{6.50}$.

We have recently developed a non-resonant broadband microwave apparatus capable of measuring the surface resistance R_s of ultra-low-loss samples continuously from 0.5 \rightarrow 22 GHz⁹. With a separate measurement of the penetration depth $\lambda(T)$ the real part of the electrical conductivity $\sigma_1(\omega, T)$ can be extracted from these data. We start with a detwinned $\text{YBa}_2\text{Cu}_3\text{O}_{6.50}$ crys-

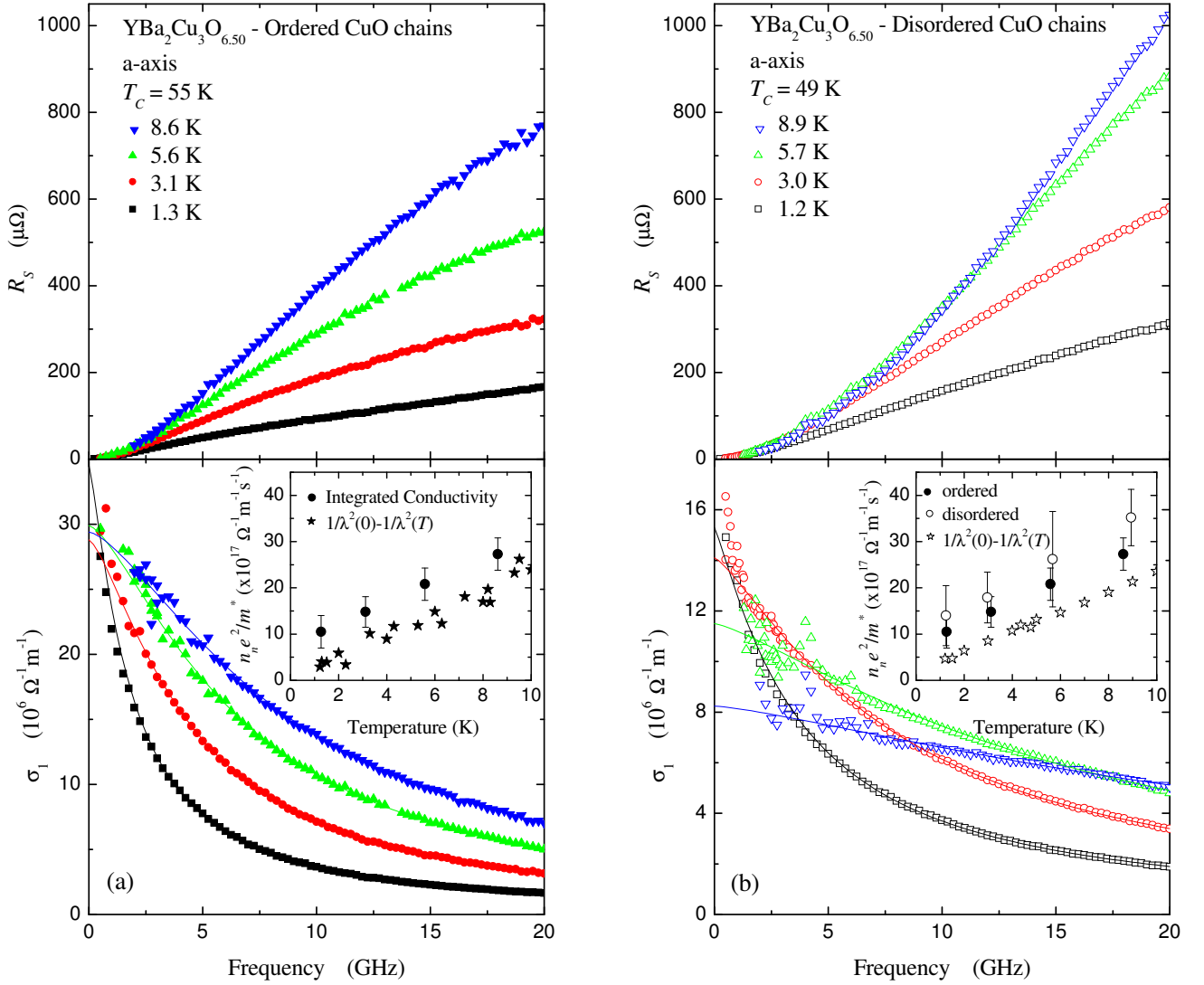


FIG. 2: (a) Top panel: Measured \hat{a} -axis surface resistance of YBa₂Cu₃O_{6.50} with highly ordered CuO chains. Bottom panel: Extracted \hat{a} -axis quasiparticle conductivity spectra. The solid lines are phenomenological fits to the data. The inset compares the oscillator strength obtained from the integrated conductivity to that obtained from $\lambda_a(T)$. (b) Top panel: Measured \hat{a} -axis R_s of YBa₂Cu₃O_{6.50} with disordered chain oxygen. Bottom panel: Extracted \hat{a} -axis quasiparticle conductivity spectra. The solid lines are phenomenological fits to the data. Inset: There is no change in the total integrated oscillator strengths before and after disordering the chain oxygen.

tal grown by the self-flux method⁶ and then annealed to achieve ordered CuO chains⁸. The temperature dependence of $\Delta\lambda(T) \equiv \lambda(T) - \lambda(1.5 \text{ K})$ was measured using a 900 MHz resonant cavity¹ and $R_s(\omega, T)$ was measured at four temperatures below 10 K using the broadband apparatus. The *same* sample was then heated to 200°C for one hour, then quenched to 0°C to reduce the order of the chain oxygen atoms, and the above measurements repeated. The sample was kept at or below 77 K for the duration of the latter measurements to prevent the degree of disorder in the CuO chains from changing.

To complete our data analysis, we use $\lambda_a(T \rightarrow 0) = 202 \pm 22 \text{ nm}$ and $\lambda_b(T \rightarrow 0) = 140 \pm 14 \text{ nm}$ for ordered YBa₂Cu₃O_{6.50} as obtained from recent zero-field ESR

measurements on Gd-doped Gd_xY_{1-x}Ba₂Cu₃O_{6+y}¹⁰. There are no reported measurements of $\lambda(T \rightarrow 0)$ for YBCO with disordered chain oxygen atoms. A reasonable estimate of these values was obtained by requiring that the low- T slope of $1/\lambda^2(T)$ remain constant upon disordering the CuO chains, as suggested by recent H_{c1} measurements on underdoped YBCO¹¹. This analysis yields $\lambda_a(T \rightarrow 0) = 238 \pm 24 \text{ nm}$ and $\lambda_b(T \rightarrow 0) = 162 \pm 16 \text{ nm}$ for disordered YBa₂Cu₃O_{6.50}. These values of $\lambda(T \rightarrow 0)$ are consistent with the relationship between T_c and $\lambda(T \rightarrow 0)$ derived from the ESR measurements on YBCO¹⁰. We emphasize that $\lambda(T \rightarrow 0)$ merely sets an overall scale factor for the $\sigma_1(\omega, T)$ spectra and its value in no way alters the key conclusions of this work.

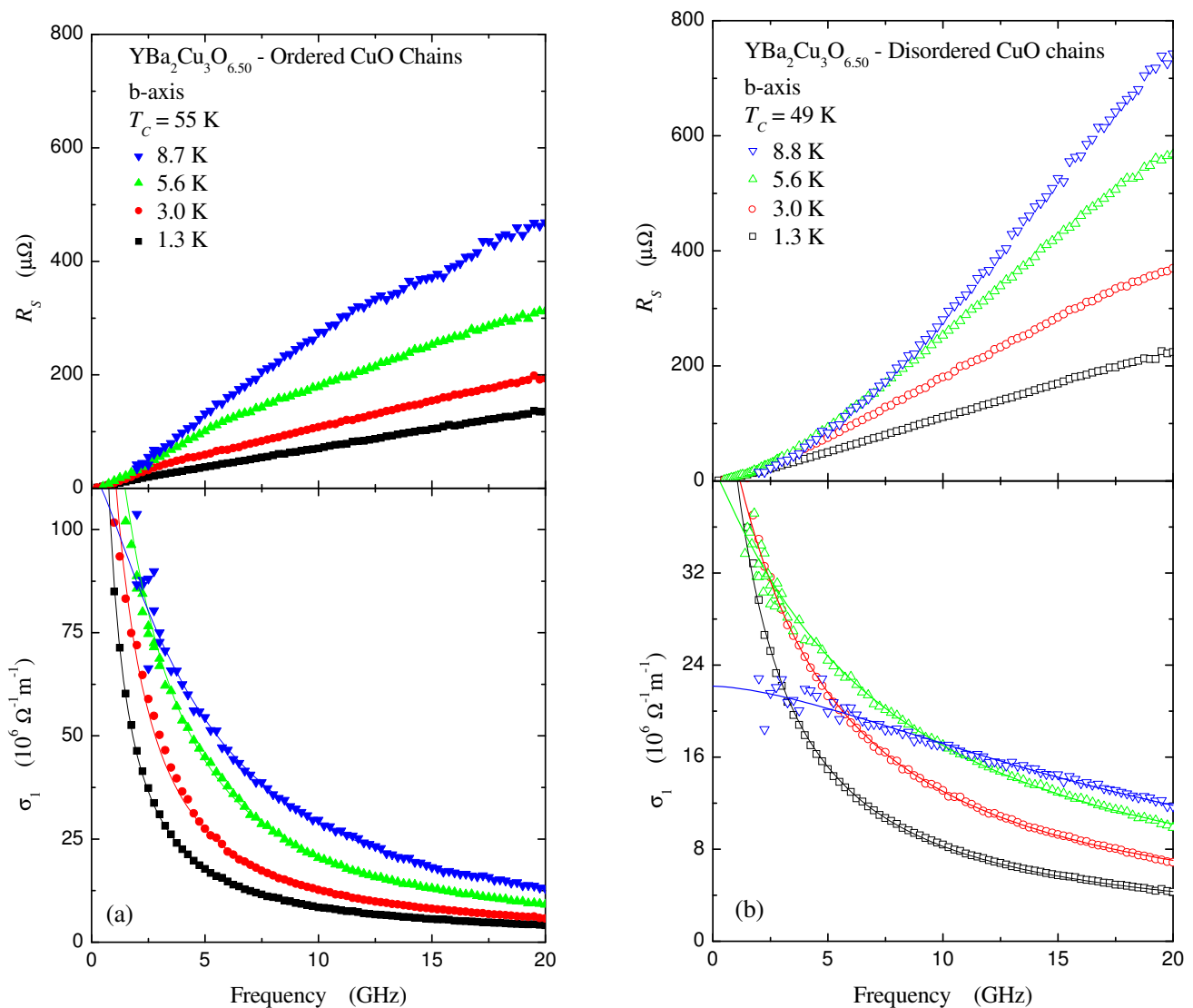


FIG. 3: (a) Top panel: Measured \hat{b} -axis R_s of YBa₂Cu₃O_{6.50} with highly ordered CuO chains. Bottom panel: Extracted \hat{b} -axis quasiparticle conductivity spectra. The solid lines are phenomenological fits to the data. (b) Top panel: Measured \hat{b} -axis R_s of YBa₂Cu₃O_{6.50} after disordering the chain oxygen. Bottom panel: Extracted \hat{b} -axis quasiparticle conductivity spectra. The solid lines are phenomenological fits to the data.

Figure 1 shows the measured change in the cavity resonant frequency $\Delta f_r(T) = f_r(1.5 \text{ K}) - f_r(T)$ due to the YBa₂Cu₃O_{6.50} sample both before and after disordering the chain oxygen atoms. The hole doping of the CuO₂ planes in YBCO is not a unique function of the oxygen content y , but depends both on y and the CuO chain ordering¹². The observed shift in T_c from 55 to 49 K upon disordering the CuO chains is due solely to a change in the hole doping of the CuO₂ planes. For $T \ll T_c$ the measured $\Delta f_r(T)$ is proportional to the change in the penetration depth $\Delta\lambda(T)$. The inset of Fig. 1 shows that $\Delta\lambda_a(T) \propto T$ for both ordered and disordered CuO chains. The measured crystal is a platelet with dimensions $\hat{a} \times \hat{b} \times \hat{c} = 0.482 \times 0.741 \times 0.028 \text{ mm}^3$. A small contribution from $\Delta\lambda_c(T)$ was removed by using

previous measurements of $\Delta\lambda_c(T)$ for a YBa₂Cu₃O_{6.60} ($T_c = 60 \text{ K}$) crystal¹³ together with the determination of the doping dependence of $\lambda_c(0)$ by Homes *et al.*¹⁴. The low- T slope of the corrected \hat{a} -axis data is $d(\Delta\lambda_a(T))/dT = 1.36 \pm 0.10 \text{ nm/K}$ which is comparable to a previously measured value of 1.05 nm/K found for a platelet with a larger $\hat{a} : \hat{c}$ aspect ratio that did not require \hat{c} -axis corrections¹⁵.

The top panel of Fig. 2a shows the measured ortho-II-ordered \hat{a} -axis surface resistance. To a very good approximation the conductivity is proportional to R_s/ω^2 and is given by $\sigma_1(\omega, T) \approx 2R_s(\omega, T)/\mu_0^2\omega^2\lambda^3(0)$. In practice, a more complete analysis that accounts for the temperature dependence of $\lambda(T)$ and self-consistently includes screening due to the quasiparticle conductivity is used

to extract σ_1 from the R_s measurements^{9,15}. The conductivity spectra obtained by the full analysis are shown in the bottom panel of Fig. 2a. These spectra are fit to a phenomenological model $\sigma_1 = \sigma_0/[1 + (\tau\omega)^y]$ which captures the observed lineshapes very well and gives a measure of the spectral width $\tau^{-1}(T)$.

As previously observed for a different sample¹⁶, the ordered $\text{YBa}_2\text{Cu}_3\text{O}_{6.50}$ conductivity data exhibit qualitative features expected for d -wave quasiparticles undergoing weak-limit scattering: cusp-like lineshapes, temperature independent $\sigma_1(\omega \rightarrow 0)$ intercepts, and T -linear spectral widths $\tau^{-1}(T)$ ¹⁵. The measured \hat{a} -axis $R_s(\omega, T)$ and $\sigma_1(\omega, T)$ after disordering the chain oxygen are shown in Fig. 2b. These conductivity spectra also have cusp-like lineshapes and T -linear $\tau^{-1}(T)$ characteristic of weak-limit scattering, however the widths of the spectra are significantly broadened. This broadening can only be attributed to increased quasiparticle scattering arising from disorder in the CuO chain layer. For completeness, in Fig. 3 we show $R_s(\omega, T)$ and $\sigma_1(\omega, T)$ for currents propagating in the \hat{b} -direction for the same $\text{YBa}_2\text{Cu}_3\text{O}_{6.50}$ sample both before and after disordering the CuO chain oxygen atoms. These data exhibit the same qualitative weak-scattering features as the \hat{a} -axis data.

In a d -wave superconductor, the linear dispersion of the energy gap sets the available phase space for quasiparticle scattering and results in a strong energy dependence of the scattering rate. For point-like defects in the limit of small scattering phase shifts, $\tau^{-1}(\epsilon) \approx 4\Gamma\epsilon/\pi\Delta_0c^2$ to within logarithmic corrections^{17,18}. Here c is the cotangent of the scattering phase shift, Δ_0 is the zero temperature superconducting gap maximum, and $\Gamma = n_i n/\pi N_0$ with n_i the concentration of defects, n the carrier density, and N_0 the density of states at the Fermi energy. In the opposite limit of large scattering phase shift, the scattering rate has a completely different energy dependence; $\tau^{-1}(\epsilon) \sim \epsilon^{-1}$. The T -linear spectral widths shown in Fig. 4 indicate that the scattering is closer to the weak limit where $\tau^{-1} \sim \epsilon$ ^{16,17}. The increased slope of $\tau^{-1}(T)$ upon disordering the CuO chains indicates that the increase in the number of oxygen chain defects corresponds to an increase in the density of weak scattering defects n_i .

The density of oxygen chain defects can be deduced from the relationship between T_c and the hole doping per Cu in the CuO_2 plane p . Using measurements of the \hat{c} -axis lattice parameter, Liang *et al.*¹² have established this relationship empirically and found it to be close to the empirical expression of Presland *et al.*¹⁹ except near $p = 1/8$. Liang's result gives $p = 0.093$ for the ordered sample with $T_c = 55$ K and $p = 0.084$ for the $T_c = 49$ K disordered sample. For oxygen ordered phases of YBCO with infinite chain lengths $p = p_0 \cdot y$ where $p_0 \approx 0.194$ ¹² is the maximum doping with all CuO chains filled. Away from perfect order, the number of holes contributed to the CuO_2 plane by a CuO chain of finite length with ℓ oxygen atoms is reduced by a factor of $(\ell - 1)/\ell$. Thus,

if the average chain has ℓ oxygen atoms the doping is given by $p \approx p_0 \cdot y \cdot (\ell - 1)/\ell$. For our sample, this analysis gives $\ell \approx 24.3$ and $\ell \approx 7.6$ before and after disordering the CuO chain oxygen respectively. Considering each chain end as a scattering defect gives a defect concentration of $n_i = 0.041$ when the sample was ordered and $n_i = 0.131$ after disordering the CuO chains. Since the slope of $\tau^{-1}(T)$ in Fig. 4 nearly triples upon disordering the CuO chains, this tripling of the oxygen defect concentration suggests that CuO chain defects are the dominant source of quasiparticle scattering even in the better ordered sample.

The conductivity calculations of Hirschfeld *et al.*^{17,18} have been extended to examine the behaviour of zero frequency intercept of the conductivity spectra in the weak scattering limit. A key result of this work is:

$$\sigma_1(\omega \rightarrow 0, T) \approx \frac{1}{2} \beta_{VC} \alpha_{FL}^2 \frac{n e^2 c^2}{m^* \Gamma},$$

where β_{VC} and α_{FL} are vertex and Fermi liquid corrections respectively²⁰. From the ordered \hat{a} -axis data the $\sigma_1(\omega \rightarrow 0)$ intercept is $30 \times 10^6 \Omega^{-1}\text{m}^{-1}$, which when combined with an estimate of $N_0 \approx 2 \times 10^{47} \text{J}^{-1}\text{m}^{-3}$ from electronic specific heat measurements of Loram *et al.*²¹ gives $\beta_{VC} \alpha_{FL}^2 c^2 \approx 2.8$. If it is assumed that the combination $\beta_{VC} \alpha_{FL}^2 \sim 1$, then the scattering phase shift is $\approx 30^\circ$, closer to the weak limit than it is to the large scattering phase shift limit.

There are other indications of intermediate scattering phase shifts in YBCO. Measurements of the \hat{a} -axis conductivity of an overdoped $\text{YBa}_2\text{Cu}_3\text{O}_{6.993}$ sample using the same broadband apparatus found that the spectra crossover from cusp-like shapes to more Lorentzian lineshapes above 4 K, indicating that this sample is best described by intermediate strength scattering¹⁶. The crossover in shape occurs because impurities with intermediate scattering strength generate a resonance in the density of states. This in turn leads to deviations from $\tau^{-1}(\epsilon) \sim \epsilon$ that become important as T increases. This view is also supported by recent thermal conductivity measurements²².

Examining the temperature dependence of the superfluid density, $\propto \lambda^{-2}(T)$, and the normal fluid density, found by integrating $\sigma_1(\omega, T)$, tests to what extent the Ferrel-Tinkham-Glover oscillator strength sum rule is obeyed. The inset of Fig. 2a shows that, to within a constant offset, the sum rule is obeyed for the ordered \hat{a} -axis data. Moreover, the inset of Fig. 2b shows that, to within experimental uncertainties, the normal fluid density is independent of CuO chain order, confirming that the increased scattering caused by CuO chain disorder is not pair-breaking (note that this particular analysis is sensitive to $\lambda(0)$). The \hat{b} -axis analysis is complicated by an additional 1-dimensional conductivity due to the CuO chains and meaningful comparisons based upon the sum rule cannot be made.

Recent attempts by Nunner and Hirschfeld to model the conductivity of BSCCO by considering off-plane

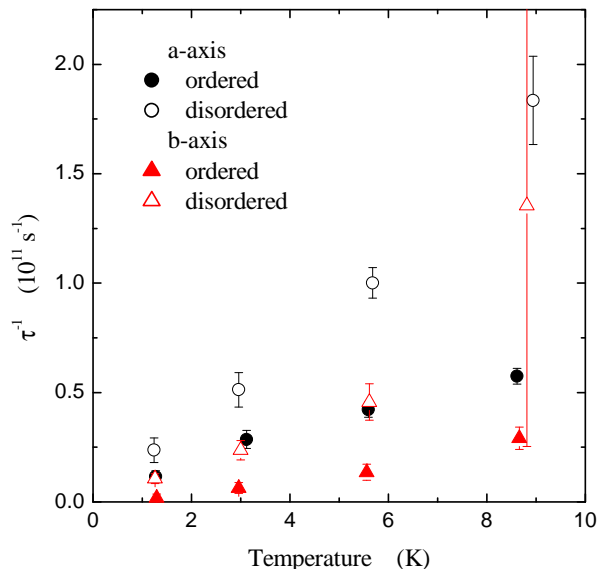


FIG. 4: Spectral width τ^{-1} versus temperature for ortho-II ordered \hat{a} -axis (solid circles) and \hat{b} -axis (solid triangles) and disordered \hat{a} -axis (hollow circles) and \hat{b} -axis (hollow triangles).

extended scatterers have been remarkably successful²³. These authors were motivated by the fact that interstitial dopant oxygen atoms and cation substitution are known sources of off-plane disorder in BSCCO. The model presented in Ref. 23 led to a plausible understanding of the temperature dependence of the quasiparticle conductivity, using defect densities typical of this material. The data sets presented here are ideal for this treatment since

the off-plane disorder dominates the quasiparticle transport, but unlike BSCCO this disorder is considerably smaller and can be easily manipulated in a single sample. It is particularly interesting to note that when Nunner and Hirschfeld allow for a significant forward-scattering component due to off-plane extended scatterers, they find that $\sigma_1(\omega, T \rightarrow 0)$ calculated is higher than the ‘universal’ limit obtained for point scatterers as $T \rightarrow 0$ and that this enhanced conductivity occurs over a wide frequency range. In other words, there is substantial oscillator strength in the conductivity spectrum that does not condense into superfluid as $T \rightarrow 0$. A similar phenomenon has been observed here in YBCO, where one finds a residual oscillator strength at 1.2 K that, while much smaller than that seen in BSCCO, is still larger than expected for point scatterers. Our measurements now unambiguously establish that in YBCO off-plane disorder associated with defected CuO chains provides the main source of weak quasiparticle scattering and forward scattering by these defects is the likely source of the small residual oscillator strength in YBCO. This material is particularly well suited to settling the controversial role that defects play in the physics of the cuprates since there is only one source of disorder; weakly-scattering oxygen defects that lie far from the CuO₂ planes.

The authors are grateful to P. J. Hirschfeld for many useful discussions throughout the course of this work. The financial support of the Natural Science and Engineering Research Council of Canada and the Canadian Institute for Advanced Research is gratefully acknowledged.

¹ W. N. Hardy, D. A. Bonn, D. C. Morgan, Ruixing Liang and Kuan Zhang, Phys. Rev. Lett. **70**, 3999 (1993).
² D. A. Bonn, S. Kamal, Kuan Zhang, Ruixing Liang, D. J. Baar, E. Klein and W. N. Hardy, Phys. Rev. B **50**, 4051 (1994).
³ S. H. Pan, E. W. Hudson, K. M. Lang, H. Eisaki, S. Uchida and J. C. Davis, Nature **403**, 746 (2000).
⁴ K. Fujita, T. Noda, K. M. Kojima, H. Eisaki and S. Uchida, Phys. Rev. Lett. **95**, 097006 (2005).
⁵ K. McElroy, Jinho Lee, J. A. Slezak, D. H. Lee, H. Eisaki, S. Uchida and J. C. Davis, Science **309**, 1048 (2005).
⁶ Ruixing Liang, W. N. Hardy, and D. A. Bonn, Physica C **304**, 105 (1998).
⁷ N. H. Andersen, M. von Zimmermann, T. Frello, M. Käll, D. Mønster, P.-A. Lindgård, J. Madsen, T. Niemöller, H. F. Poulsen, O. Schmidt, J. R. Schneider, Th. Wolf, P. Dosanjh, R. Liang, and W. N. Hardy, Physica C **317-318**, 259 (1999).
⁸ Ruixing Liang, W. N. Hardy, and D. A. Bonn, Physica C **336**, 57 (2000).
⁹ P. J. Turner, D. M. Broun, Saeid Kamal, M. E. Hayden, J. S. Bobowski, R. Harris, D. C. Morgan, J. S. Preston, D. A. Bonn, and W. N. Hardy, Rev. Sci. Instrum **75**, 124 (2004).

¹⁰ T. Pereg-Barnea, P. J. Turner, R. Harris, G. K. Mullins, J. S. Bobowski, M. Raudsepp, R. Liang, D. A. Bonn, and W. N. Hardy, Phys. Rev. B **69**, 184513 (2004).
¹¹ Ruixing Liang, D. A. Bonn, W. N. Hardy, and David Broun, Phys. Rev. Lett. **94**, 117001 (2005).
¹² Ruixing Liang, D. A. Bonn, and W. N. Hardy, Phys. Rev. B **73**, 180505 (2006).
¹³ D. A. Bonn, S. Kamal, A. Bonakdarpour, Ruixing Liang, W. N. Hardy, C. C. Homes, D. N. Basov and T. Timusk, Czech. J. Phys. **46**, 3195 (1996).
¹⁴ C. C. Homes, T. Timusk, D. A. Bonn, R. Liang, and W. N. Hardy, Physica C **254**, 265 (1995).
¹⁵ P. J. Turner, R. Harris, Saeid Kamal, M. E. Hayden, D. M. Broun, D. C. Morgan, A. Hosseini, P. Dosanjh, G. K. Mullins, J. S. Preston, Ruixing Liang, D. A. Bonn, and W. N. Hardy, Phys. Rev. Lett. **90**, 237005 (2003).
¹⁶ R. Harris, P. J. Turner, Saeid Kamal, A. R. Hosseini, P. Dosanjh, G. K. Mullins, J. S. Bobowski, C. P. Bidnost, D. M. Broun, Ruixing Liang, W. N. Hardy and D. A. Bonn, Phys. Rev. B **74**, 104508 (2006).
¹⁷ P. J. Hirschfeld, W. O. Putikka and D. J. Scalapino, Phys. Rev. Lett. **71**, 3705 (1993).
¹⁸ P. J. Hirschfeld, W. O. Putikka and D. J. Scalapino, Phys. Rev. B **50**, 10250 (1994).

- ¹⁹ M. R. Presland, J. L. Tallon, R. G. Buckley, R. S. Liu, and N. E. Flower, *Physica C* **176**, 95 (1991).
- ²⁰ R. Harris, Ph.D. thesis, University of British Columbia (2004).
- ²¹ J. W. Loram, K. A. Mirza, J. R. Cooper and W. Y. Liang, *Phys. Rev. B* **71**, 1740 (1993).
- ²² R. W. Hill, Christian Lupien, M. Sutherland, Etienne Boaknin, D. G. Hawthorn, Cyril Proust, F. Ronning, Louis Taillefer, Ruixing Liang, D. A. Bonn and W. N. Hardy, *Phys. Rev. Lett.* **92**, 027001-1 (2004).
- ²³ Tamara S. Nunner and P. J. Hirschfeld, *Phys. Rev. B* **72**, 014514 (2005).